Simulation Study of High-Frequency Pulsed DC Discharges in Nitrogen

Lizhu Tong
Keisoku Engineering System Co., Ltd.
1-9-5 Uchikanda, Chiyoda-ku, Tokyo 101-0047, Japan, tong@kesco.co.jp

Abstract: Pulsed DC technology has led to the design of cost-effective deposition systems and to improved film properties, compared to conventional rf systems. In this work, a two-dimensional finite element model is used to investigate the high frequency pulsed DC discharges in nitrogen. The study is performed using the Plasma Module of COMSOL Multiphysics@. The densities of all the plasma species are obtained. The temporal evolutions of averaged electron density, averaged electron temperature, and averaged densities of ions and neutrals are presented. The effects of pulse frequencies and duty cycle ratios on plasma properties are examined.

Keywords: Pulsed DC discharge, High frequency, Nitrogen, Numerical simulation.

1. Introduction

Pulsed plasmas exhibit improved etching and deposition rates, reduced formation of dust particles, and uniformity of deposition [1]. Controls of the plasma chemistry, electron energy distributions and plasma characteristics have been obtained by adjusting the pulse repetition frequency and duty cycle ratio of the pulsed power in inductively coupled methane plasmas and capacitively coupled Ar and Ar/CF_4/O_2 plasmas [2,3].

Pulsed DC technology may reduce powder formation and allow more precise control of the generation of reactive species. This technology has permitted the development of more sophisticated equipment with ionization sources and has led to the production of innovative materials [4-7]. Recently, time-resolved measurements of electron density in pulsed DC discharges in nitrogen and argon operating at the pulse frequency of 0.4~25 kHz have been reported [8]. Although a bi-Maxwellian electron energy distribution was proposed, the plasma properties in these discharges such as the temporal evolutions of electron temperature and densities of the species contributing to metal nitridation were not obtained. In the present work, an extensive simulation study of high frequency pulsed DC glow discharges is performed by using COMSOL Multiphysics@. The spatiotemporal distributions of plasma species are obtained and the pulsed DC plasma properties are discussed.

2. Numerical Model

The research is conducted in a DC glow discharge device designed for metal nitridation [8]. Gas is nitrogen. The gas pressure is 10 Pa. A negative high voltage of –2 kV at the pulse repetition frequency of 1 or 10 kHz is connected to the cathode (diameter=13 cm) through a series RC circuit comprised of a ballast resistor of 100 Ω and a blocking capacitor of 50 nF. The model includes an axisymmetric discharge area of 15×20 cm^2 size. The cathode center is located at r = 0 cm and z = −5 cm. The centers of grounded anodes (30×30 cm^2) are located at r=15 cm and z=15 cm. The duty cycle ratios (discharge ON time/ discharge pulse period, DCR) are 25% and 50%.

The species taken into account are electrons, ions (N_2^+, N_4^+, N^+), neutrals in ground state (N_2, N), and neutrals in excited state ($N_2(A^3\Sigma_u^+)$, N_2 ($B^3\Pi_g$), N_2 ($B'\,^3\Sigma_u^-$), N_2 ($a'\,^1\Sigma_u^-$), N_2 ($a\,^1\Pi_g$), N_2 ($w\,^1\Delta_u$), N_2 ($C\,^3\Pi_u$)), as shown in Table 1. The chemical reactions, in which the electron-induced collisions, the reactions of ions by collisions with atoms and molecules, the reactions of excited nitrogen molecules by collisions with atoms and molecules, and the photoemissions are included, are listed in Tables 2 [9]. The basic equations of the plasma simulations used in this research include a pair of drift–diffusion equations for the electrons, a modified Maxwell–Stefan equation for the ion and neutral species, and a Poisson's equation for the space charge electric field. Since a pulsed DC voltage is used, the secondary electron emission due to ion impact becomes a significant factor to sustain the pulsed discharge. In this work, the secondary electron emission coefficient is set to 0.25. Ions are considered as completely absorbed/neutralized when they arrive at the electrodes. The excited nitrogen molecules

Table 1: The species included in the model.

Neutrals	Neutrals in excited state	Ions	electrons
N_2, N	$N_2(A\ ^3\Sigma_u^+)$/$N_2(A)$ $N_2(B\ ^3\Pi_g)$/$N_2(B)$ $N_2(B'\ ^3\Sigma_u^-)$/$N_2(B')$ $N_2(a'\ ^1\Sigma_u^-)$/$N_2(a')$ $N_2(a\ ^1\Pi_g)$/$N_2(a)$ $N_2(w\ ^1\Delta_u)$/$N_2(w)$ $N_2(C\ ^3\Pi_u)$/$N_2(C)$	N^+, N_2^+, N_4^+	e^-

Table 2: The chemical reactions included in the model (ε: electron energy).

No.	Reaction	Rate coefficient ($s^{-1}/cm^3\cdot s^{-1}/cm^6\cdot s^{-1}$)
1	$e^- + N_2 \rightarrow e^- + N_2$	$f(\varepsilon)$
2	$e^- + N_2 \rightarrow e^- + N_2(A)$	$f(\varepsilon)$
3	$e^- + N_2 \rightarrow e^- + N_2(B)$	$f(\varepsilon)$
4	$e^- + N_2 \rightarrow e^- + N_2(B')$	$f(\varepsilon)$
5	$e^- + N_2 \rightarrow e^- + N_2(a')$	$f(\varepsilon)$
6	$e^- + N_2 \rightarrow e^- + N_2(a)$	$f(\varepsilon)$
7	$e^- + N_2 \rightarrow e^- + N_2(w)$	$f(\varepsilon)$
8	$e^- + N_2 \rightarrow e^- + N_2(C)$	$f(\varepsilon)$
9	$e^- + N_2 \rightarrow 2e^- + N_2^+$	$f(\varepsilon)$
10	$e^- + N_2 \rightarrow 2e^- + N^+ + N$	$f(\varepsilon)$
11	$e^- + N \rightarrow 2e^- + N^+$	$f(\varepsilon)$
12	$e^- + N_2^+ \rightarrow N + N$	$4.8\times10^{-7}(300/T_e)^{0.5}$
13	$e^- + N_4^+ \rightarrow N_2 + N_2$	$2.0\times10^{-6}(300/T_e)^{0.5}$
14	$N^+ + N_2 \rightarrow N + N_2^+$	4.45×10^{-10}
15	$N_2^+ + N \rightarrow N_2 + N^+$	$2.4\times10^{-15}T_g$
16	$N_4^+ + N_2 \rightarrow N_2^+ + N_2 + N_2$	$2.1\times10^{-16}\exp(T_g/121)$
17	$N_4^+ + N \rightarrow N^+ + N_2 + N_2$	10^{-11}
18	$N_2(A) + N_2(A) \rightarrow N_2(B) + N_2$	7.7×10^{-11}
19	$N_2(A) + N_2(A) \rightarrow N_2(C) + N_2$	1.5×10^{-10}
20	$N_2(A) + N \rightarrow N_2 + N$	4.0×10^{-11}
21	$N_2(A) + N_2(a') \rightarrow N_4^+ + e^-$	9.0×10^{-12}
22	$N_2(A) + N_2(a') \rightarrow N_2^+ + N_2 + e^-$	1.0×10^{-12}
23	$N_2(B) + N_2 \rightarrow N_2(A) + N_2$	2.85×10^{-11}
24	$N_2(B) + N_2 \rightarrow N_2 + N_2$	1.5×10^{-12}
25	$N_2(B) \rightarrow N_2(A) + h\nu$	2.0×10^{5}
26	$N_2(a') + N_2 \rightarrow N_2(B) + N_2$	1.9×10^{-13}
27	$N_2(a') + N_2(a') \rightarrow N_4^+ + e$	4.5×10^{-11}
28	$N_2(a') + N_2(a') \rightarrow N_2^+ + N_2 + e^-$	5.0×10^{-12}
29	$N_2(a) + N_2 \rightarrow N_2(a') + N_2$	2.2×10^{-11}
30	$N_2(a) \rightarrow N_2 + h\nu$	1.7×10^{4}
31	$N_2(a) \rightarrow N_2(a') + h\nu$	1.91×10^{4}
32	$N_2(w) + N_2 \rightarrow N_2(a) + N_2$	1.0×10^{-11}
33	$N_2(w) \rightarrow N_2(a) + h\nu$	6.4×10^{2}
34	$N_2(C) \rightarrow N_2(B) + h\nu$	2.74×10^{7}

are set to revert to their ground states when they contact with the walls. The surface loss of N atoms is given by $R = -\left(\frac{\gamma}{1-\gamma/2}\right)\frac{v}{4}c$, where c is the density of atom N, $v = \sqrt{8k_BT/\pi m}$ is the average velocity of the N atoms, where k_B is the Boltzmann constant, T is the temperature, and m is the mass of atom N. γ is the surface loss probability, which is set to 0.07 in this work [10].

3. Simulation results

Figure 1 shows the calculated results for a pulsed DC plasma at the pulse frequency of 1 kHz and 25% DCR. As the temporal evolution of pulsed DC voltage, the electron density, electron temperature, and densities of ions and neutrals appear the pulse variations. The pulse amplitude of averaged electron density is $1.9\times10^{15}\,\mathrm{m}^{-3}$. The maximum averaged electron temperature is

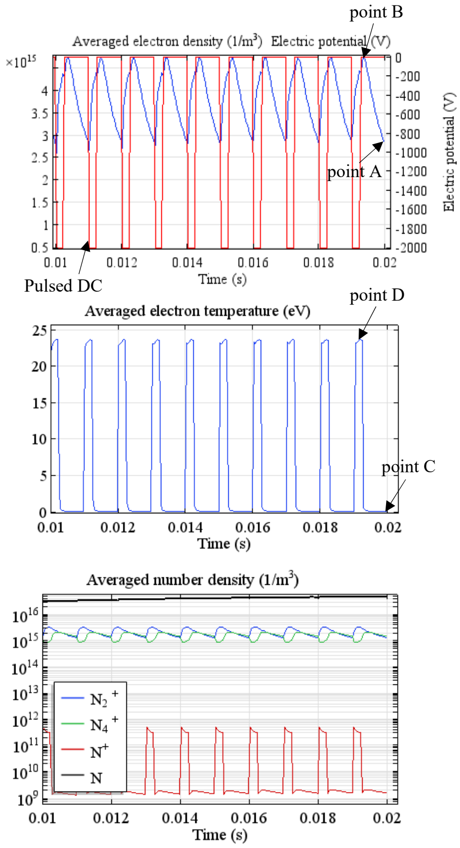

Figure 1. Temporal evolutions of averaged electron density, averaged electron temperature, and averaged densities of ions and neutrals in a pulsed DC plasma at the pulse frequency of 1 kHz and 25% DCR.

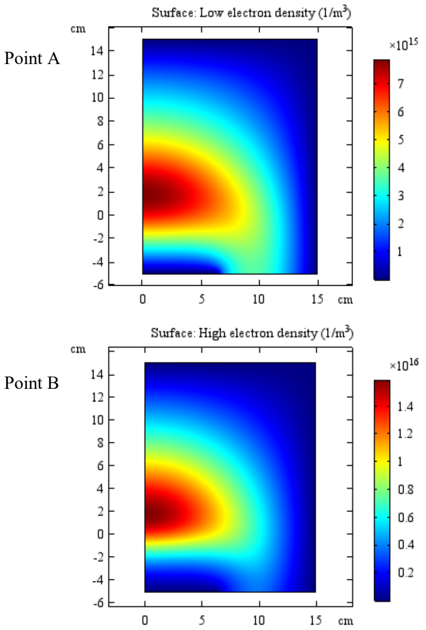

(a) Low electron density (Point A) and high electron density (point B)

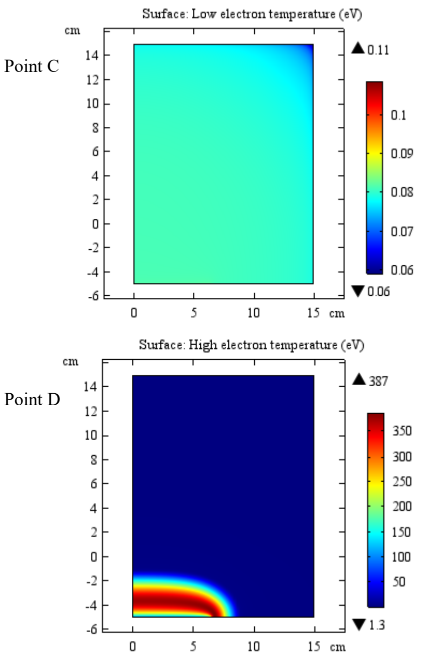

(b) Low electron temperature (Point C) and high electron temperature (point D)

Figure 2. Electron density and electron temperature at the different time points in a pulsed DC plasma at the pulse frequency of 1 kHz and 25% DCR.

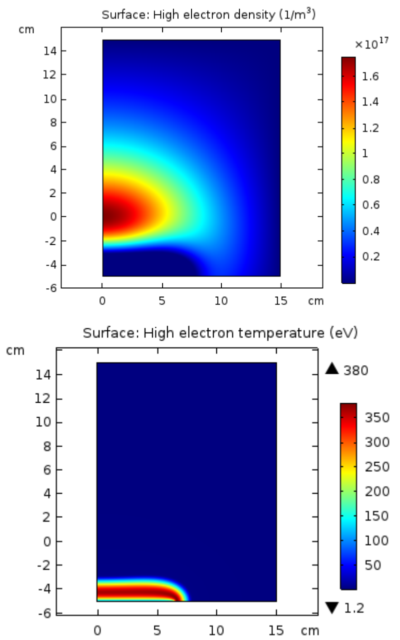

Figure 3. High electron density and high electron temperature in a pulsed DC plasma at the pulse frequency of 1 kHz and 50% DCR.

is 23.7 eV. The densities of N_2^+ and N_4^+ are much higher than that of N^+ that appears a large pulse variation. The density of atom N gradually increases.

Figure 2 shows the electron density and electron temperature at the different time points as shown in Fig. 1. The high electron density at the time point B presents more intensive across the symmetrical axis than the low electron density at the time point A. The electron temperature over the cathode at the maximum amplitude of pulse voltage appears extremely high, arriving at a maximum value of 387 eV. On the contrary, when the pulse voltage value is changed to zero, the electron temperature becomes very low over all the plasma area. Results at the pulse frequency of 1 kHz and 50% DCR show a similar tendency, but the electron density is much higher and more intensive. Although the maximum electron temperature is not increased, the high electron temperature is concentrated to the cathode. It can be deduced to a fact that the increase of electron density causes the plasma sheath in contact with the electrode to be thinner. The maximum electron density increases from $1.59 \times 10^{16} \mathrm{m}^{-3}$ of 25% DCR to $1.75 \times 10^{17} \mathrm{m}^{-3}$ of 50% DCR.

The calculated results at the pulse frequency

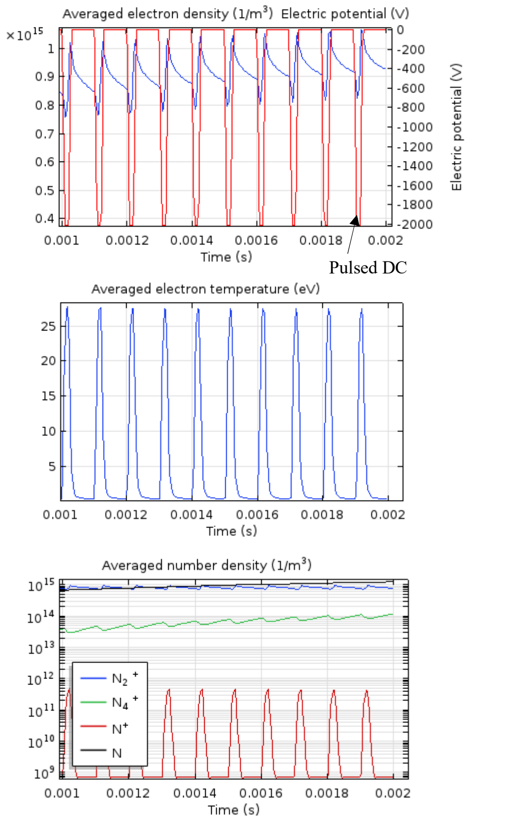

Figure 4. Temporal evolutions of averaged electron density, averaged electron temperature, and averaged densities of ions and neutrals in a pulsed DC plasma at the pulse frequency of 10 kHz and 25% DCR.

of 10 kHz and 25% DCR are shown in Fig. 4. Due to the increase of the pulse frequency, the electron density is evidently reduced and the time period with high electron temperature becomes narrow. The effect of the external series RC circuit on the pulsed DC discharge is also presented in the variation of the pulsed DC, which may be regarded as the charge-discharge effect of the blocking capacitor. The density of N_2^+ is one order higher than that of N_4^+. N^+ appears a pulse variation similar to that at the low pulse frequency, but the high density area is narrower.

4. Conclusions

This paper presents the simulation results of the high frequency pulsed DC discharges in nitrogen. 13 kinds of plasma species including electrons, ions and neutrals as well as 34 kinds of chemical reactions are considered. The pulsed plasma properties are obtained. The extremely high electron temperature is shown over the cathode at the maximum amplitude of pulse voltage. The increase of DCR causes the electron density to rise rapidly. Contrarily, an increase of the pulse frequency causes the electron density to go down.

5. References

1. P. Subramonium and M.J. Kushner, "Pulsed plasmas as a method to improve uniformity during materials processing", *J. Appl. Phys.*, **96**, 82-93 (2004)
2. M. Bauer, T. S.-Selinger, H. Kang, and A. von Keudell, "Control of the plasma chemistry of a pulsed inductively coupled methane plasma", *Plasma Sources Sci. Technol.* **14**, 543–548 (2005)
3. S.-H. Song and M.J. Kushner, "Control of electron energy distributions and plasma characteristics of dual frequency, pulsed capacitively coupled plasmas sustained in Ar and $Ar/CF_4/O_2$", *Plasma Sources Sci. Technol.*, **21**, 055028 (2012)
4. C. Corbella, M. Rubio-Roy, E. Bertran, and J.L. Andújar, "Plasma parameters of pulsed-dc discharges in methane used to deposit diamond-like carbon films", *J. Appl. Phys.*, **106**, 033302 (2009)
5. D. Lundin, J. Jensen, and H. Pedersen, "Influence of pulse power amplitude on plasma properties and film deposition in high power pulsed plasma enhanced chemical vapor deposition", *J. Vac. Sci. Technol. A*, **32**, 030602 (2014)
6. F.L. Wen, Y.L. Lo, C.H. Lin, and S.C. Mou, "A pulse DC plasma deposited resistor process," *Mater. Sci. Forum*, **505-507**, 865-870 (2006)
7. D. Gahan, S. Daniels, C. Hayden, P. Scullin, D. O'Sullivan, Y.T. Pei and M.B. Hopkins, "Ion energy distribution measurements in rf and pulsed dc plasma discharges", *Plasma Sources Sci. Technol.*, **21**, 024004 (2012)
8. A. Pandey, W. Sakakibara, H. Matsuoka, K. Nakamura, and H. Sugai, "Time-resolved curling-probe measurements of electron density in high frequency pulsed DC discharges", *Jpn. J. Appl. Phys.*, **55**, 016101 (2016)
9. L.Z. Tong, "Numerical study of the effect of gas flow in low pressure inductively coupled Ar/N_2 plasmas", *Cent. Eur. J. Phys.*, **10**, 888-897 (2012)
10. L.Z. Tong, "Study of low pressure inductively coupled plasmas: Effects of the DC bias and gas flow rate", *Jpn. J. Appl. Phys.*, **52**, 05EA03 (2013)